

Movement Properties of Antiresonance Vibration Mill with Symmetrical Construction

Grzegorz CIEPŁOK

*AGH University of Science and Technology, al. Mickiewicza 30, 30-059 Kraków,
cieplok@agh.edu.pl*

Paweł PIEKAJ

*AGH University of Science and Technology, al. Mickiewicza 30, 30-059 Kraków,
piekaj@agh.edu.pl*

Abstract

Vibration mills used in the industry are an alternative to conventional gravity mills. Compared to gravity mills they have much lower demand for energy of the milling process, significantly lower mass and several times lower cost of raw materials milling. In addition, they have much greater technological possibilities, which justifies their use in many cases. Apart from a number of advantages, vibration mills have disadvantages. The dynamics of work causes a significant transfer of vibrations to the ground and a major load on the vibrator bearings. As a result, they require temperature monitoring and the use of complex cooling systems. It is possible to reduce these negative effects by using new construction solutions.

Keywords: vibration mill, vibration grinding, antiresonance.

1. Introduction

From the beginning of the XX century a constant increase of requirements for grained materials, including materials formed in the milling process, is observed. In effect, there is a constant increase of requirements for mills of higher and higher efficiency. The focus of this study is the new solution of vibration mills constituting certain alternative for gravity mills. In these mills the kinetic energy of free grinding media (usually ball-shaped) and intensity of interactions between them and with the milled material, depends on the acceleration of gravity and dimensions of the mill chamber. The kinetic energy of grinding media in vibration mills is transferred from the vibrating chamber. This energy, as well as the intensity of grinding media interactions, depends on motion parameters of the chamber, i.e. on its frequency, vibration amplitude and trajectory, which - in turn - depends on the mill designer and user [1].

Vibration mills are known for more than 100 years and during these years they were intensely developed. Presently the most often used are overresonance tube mills of the inertial excitation and circular or elliptical trajectory of the chamber movement [1, 2, 3]. These mills are having chambers of a capacity up to 100 m³ and the power of up to 2 MW, and are applied in a majority of powders production technologies. The main advantages of vibration mills as compared with gravity mills, are much wider technological possibilities. They allow to achieve: much finer granulation, lower energy demand for milling process (4 - 10 times), lower cost of grinding media (6 - 8 times), smaller mass and smaller building area required. However, apart from advantages, these

mills have also disadvantages, such as a strong influence on the ground and major load on bearings of inertial vibrators, which - in turn - force monitoring of their temperature and application of complex cooling systems [1]. There is a possibility of reducing these negative effects by applications of new solutions.

The proposed solution constitutes the mill, which operations are based on the antiresonance effect. This antiresonance mill, in contrast to the currently applied mills of a similar construction [4], allows to obtain a circular trajectory of the chamber movement and a better chamber filling coefficient. The utilisation of the antiresonance allows to reduce forces transferred on the foundations and making drive units smaller [5]. An attempt to decrease negative influences of mills on the environment at the situation of increasing demands for larger and larger mills, seems justified and therefore was undertaken in this study. Investigations related to the development of this type of mills were divided into several stages. In this study, the pressure is directed to the mathematical model of the mill, being the base of its movements analysis. Differential equations of mill movements were determined and the simulation results were verified by measurements on the laboratory research set-up, shown in Figure 1.

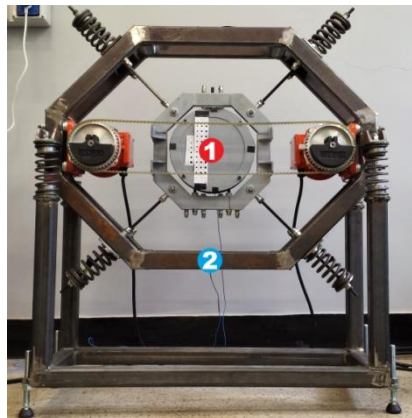


Figure 1. Research set-up with marked places of mounting accelerometers on:
1 – chamber, 2 – frame

Both theoretically and experimentally the efficiency of operations of the solution, was revealed. Very promising results were achieved, especially in the scope of reducing undesired influences and the stability of chamber operations at the set vibrations level, as well as at maintaining the circular motion trajectory.

2. Mathematical model of the antiresonance vibration mill

The scheme of the antiresonance vibration mill, shown in the photograph in the introduction, is presented in Figure 2. It consists of a stiff metal frame placed on the steel springs system excited for vibrations by means of two inertial vibrators. The system of four symmetrically distributed rods is mounted by joints to the frame. These rods are elastically connected with the chamber, by means of coil springs, and are transferring the

frame vibrations to this chamber. In such way the symmetric system of two centrally placed bodies connected by elastic elements with each other and with the foundation, is formed. The frame antiresonance, resulting from the possibility of zeroing the sum of forces influencing the frame by inertial vibrators and by the chamber, is possible in this system.

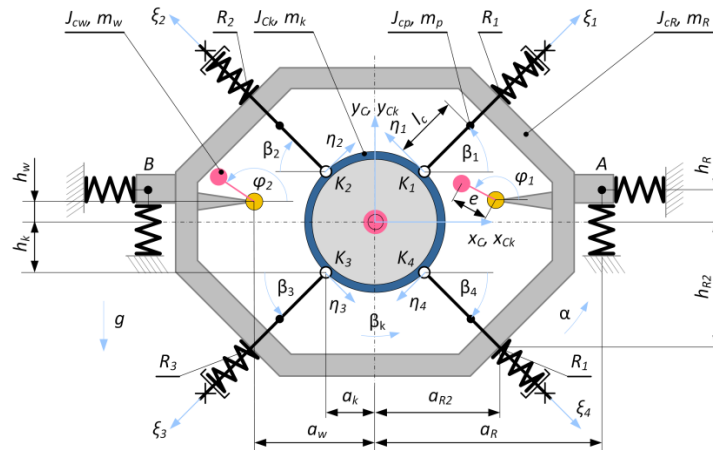


Figure 2. Scheme of the antiresonance vibration mill

The system presented in Figure 2 has 12 degrees of freedom. It can be described by 3 coordinates: x_C, y_C, α - describing the frame motion, 3 coordinates: x_{Ck}, y_{Ck}, β - describing the chamber motion, 4 coordinates: $\beta_1, \beta_2, \beta_3, \beta_4$ - describing angular displacements of rods and 2 coordinates: φ_1, φ_2 - describing angular displacements of inertial vibrators.

Dynamic equations of motion of the system were derived on the basis of the Lagrangian Method of the II kind. However, in consideration of their extended form and limited volume of the hereby paper, only the most important element of their derivation, i.e. the Lagrangian function is included. Such approach provides - for readers - a possibility to recognize the accuracy of the model as well as an opportunity to determine these equations by themselves.

In order to determine the Lagrangian function, understood as the difference of a kinetic and potential energy of the system, the geometric dependences were formulated. These dependencies allowed, on the one side to determine mass velocities of individual parts of the system and on the other side to determine deformations of elastic elements.

A potential energy contained in elastic elements can be presented in a form:

$$\begin{aligned}
 V = & \frac{1}{2} k_{\xi_1} \delta_{\xi_1}^2 + \frac{1}{2} k_{\xi_2} \delta_{\xi_2}^2 + \frac{1}{2} k_{\xi_3} \delta_{\xi_3}^2 + \frac{1}{2} k_{\xi_4} \delta_{\xi_4}^2 + \frac{1}{2} k_{\eta_1} \delta_{\eta_1}^2 + \frac{1}{2} k_{\eta_2} \delta_{\eta_2}^2 + \frac{1}{2} k_{\eta_3} \delta_{\eta_3}^2 \\
 & + \frac{1}{2} k_{\eta_4} \delta_{\eta_4}^2 + \frac{1}{2} k_{xR} \delta_{x_A}^2 + \frac{1}{2} k_{xR} \delta_{x_B}^2 + \frac{1}{2} k_{yR} \delta_{y_A}^2 + \frac{1}{2} k_{yR} \delta_{y_B}^2
 \end{aligned} \tag{1}$$

where: $\delta\check{\xi}_i, \delta\check{\eta}_i$ denote elongations of chamber springs along the longitudinal ξ and transverse η axis, respectively. These displacements can be determined from dependences:

$$\delta_{\xi_1} = (x_{K1} - x_{R1}) \cos \beta_1 + (y_{K1} - y_{R1}) \sin \beta_1 \tag{2}$$

$$\delta_{\xi_2} = (x_{K2} - x_{R2}) \cos \beta_2 + (y_{K2} - y_{R2}) \sin \beta_2 \tag{3}$$

$$\delta_{\xi_3} = (x_{K3} - x_{R3}) \cos \beta_3 + (y_{K3} - y_{R3}) \sin \beta_3 \tag{4}$$

$$\delta_{\xi_4} = (x_{K4} - x_{R4}) \cos \beta_4 + (y_{K4} - y_{R4}) \sin \beta_4 \tag{5}$$

$$\delta_{\eta_1} = (x_{K1} - x_{R1}) \sin \beta_1 + (y_{K1} - y_{R1}) \cos \beta_1 + l_p(\beta_1 - \beta_0) \tag{6}$$

$$\delta_{\eta_2} = (x_{K2} - x_{R2}) \sin \beta_2 + (y_{K2} - y_{R2}) \cos \beta_2 + l_p(\beta_2 - \beta_0) \tag{7}$$

$$\delta_{\eta_3} = (x_{K3} - x_{R3}) \sin \beta_3 + (y_{K3} - y_{R3}) \cos \beta_3 + l_p(\beta_3 - \beta_0) \tag{8}$$

$$\delta_{\eta_4} = (x_{K4} - x_{R4}) \sin \beta_4 + (y_{K4} - y_{R4}) \cos \beta_4 + l_p(\beta_4 - \beta_0) \tag{9}$$

where: $x_{Ki}, y_{Ki}, x_{Ri}, y_{Ri}$ displacements of the clamping points of springs to the chamber (10)-(17) and to the frame (18)-(25), respectively.

$$x_{K1} = x_{Ck} - \beta_k h_k \tag{10}$$

$$y_{K1} = y_{Ck} + a_k \beta_k \tag{11}$$

$$x_{K2} = x_{Ck} - \beta_k h_k \tag{12}$$

$$y_{K2} = y_{Ck} - a_k \beta_k \tag{13}$$

$$x_{K3} = x_{Ck} + \beta_k h_k \tag{14}$$

$$y_{K3} = y_{Ck} - a_k \beta_k \tag{15}$$

$$x_{K4} = x_{Ck} + \beta_k h_k \tag{16}$$

$$y_{K4} = y_{Ck} + a_k \beta_k \tag{17}$$

$$x_{R1} = x_C - h_{R2} \alpha \tag{18}$$

$$y_{R1} = y_C + a_{R2} \alpha \tag{19}$$

$$x_{R2} = x_C - h_{R2} \alpha \tag{20}$$

$$y_{R2} = y_C - a_{R2} \alpha \tag{21}$$

$$x_{R3} = x_C + h_{R2} \alpha \tag{22}$$

$$y_{R3} = y_C - a_{R2} \alpha \tag{23}$$

$$x_{R4} = x_C + h_{R2} \alpha \tag{24}$$

$$y_{R4} = y_C + a_{R2} \alpha \tag{25}$$

In turn, elongations of springs of the frame suspension in the longitudinal y and transverse x directions can be determined from dependences (26)-(29).

$$\delta_{x_A} = x_C - h_R \alpha \tag{26}$$

$$\delta_{x_B} = x_C - h_R \alpha \tag{27}$$

$$\delta_{y_A} = y_C + a_R \alpha \tag{28}$$

$$\delta_{y_B} = y_C - a_R \alpha \tag{29}$$

The kinetic energy of the system is determined by the sum of the kinetic energy of the frame (30), chamber (31) and four rods (32).

$$\begin{aligned}
E_{ramy} = & \frac{1}{2}m_w(\dot{x}_C - \dot{\varphi}_1 e \sin(\varphi_1))^2 + \frac{1}{2}m_w(a_w \dot{\alpha} + \dot{y}_C + \dot{\varphi}_1 e \cos(\varphi_1))^2 \\
& + \frac{1}{2}m_w(\dot{x}_C - \dot{\varphi}_2 e \sin(\varphi_2))^2 \\
& + \frac{1}{2}m_w(-a_w \dot{\alpha} + \dot{y}_C + \dot{\varphi}_2 e \cos(\varphi_2))^2 + \frac{1}{2}J_{cw}\dot{\varphi}_1^2 + \frac{1}{2}J_{cw}\dot{\varphi}_2^2 \\
& + \frac{1}{2}m_R \dot{x}_C^2 + \frac{1}{2}m_R \dot{y}_C^2 + \frac{1}{2}J_{cR} \dot{\alpha}^2
\end{aligned} \quad (30)$$

$$E_{kom} = \frac{1}{2}m_k \dot{y}_{Ck}^2 + \frac{1}{2}m_k \dot{x}_{Ck}^2 + J_{Ck} \dot{\beta}_k^2 \quad (31)$$

$$\begin{aligned}
E_{pret} = & \frac{1}{2}m_p \dot{x}_{C1}^2 + \frac{1}{2}m_p \dot{y}_{C1}^2 + \frac{1}{2}J_{cp} \dot{\beta}_1^2 + \frac{1}{2}m_p \dot{x}_{C2}^2 + \frac{1}{2}m_p \dot{y}_{C2}^2 + \frac{1}{2}J_{cp} \dot{\beta}_2^2 \\
& + \frac{1}{2}m_p \dot{x}_{C3}^2 + \frac{1}{2}m_p \dot{y}_{C3}^2 + \frac{1}{2}J_{cp} \dot{\beta}_3^2 + \frac{1}{2}m_p \dot{x}_{C4}^2 + \frac{1}{2}m_p \dot{y}_{C4}^2 \\
& + \frac{1}{2}J_{cp} \dot{\beta}_4^2
\end{aligned} \quad (32)$$

where:

$$\dot{x}_{C1} = \dot{x}_{Ck} - h_k \dot{\beta}_k - l_c \sin(\beta_1) \dot{\beta}_1 \quad (33)$$

$$\dot{y}_{C1} = \dot{y}_{Ck} + a_k \dot{\beta}_k + l_c \cos(\beta_1) \dot{\beta}_1 \quad (34)$$

$$\dot{x}_{C2} = \dot{x}_{Ck} - h_k \dot{\beta}_k + l_c \sin(\beta_2) \dot{\beta}_2 \quad (35)$$

$$\dot{y}_{C2} = \dot{y}_{Ck} - a_k \dot{\beta}_k + l_c \cos(\beta_2) \dot{\beta}_2 \quad (36)$$

$$\dot{x}_{C3} = \dot{x}_{Ck} + h_k \dot{\beta}_k + l_c \sin(\beta_3) \dot{\beta}_3 \quad (37)$$

$$\dot{y}_{C3} = \dot{y}_{Ck} - a_k \dot{\beta}_k - l_c \cos(\beta_3) \dot{\beta}_3 \quad (38)$$

$$\dot{x}_{C4} = \dot{x}_{Ck} + h_k \dot{\beta}_k - l_c \sin(\beta_4) \dot{\beta}_4 \quad (39)$$

$$\dot{y}_{C4} = \dot{y}_{Ck} + a_k \dot{\beta}_k - l_c \cos(\beta_4) \dot{\beta}_4 \quad (40)$$

Table 1. Parameters of the mill model

Parameters of the mill model								
Chamber parameters			Frame parameters			Elastic support of the frame		
J_{cp}	kg·m ²	0.0086	m_R	kg	45.11	k_{xR}	N/m	5554.1
J_{ck}	kg·m ²	0.163	m_w	kg	4.08	k_{yR}	N/m	21114.5
m_k	kg	8.95	e	mm	4.6	b_{xR}	N·s/m	11.2
m_p	kg	0.25	a_w	mm	335	b_{yR}	N·s/m	21.85
a_k	mm	115	h_w	mm	0	Elastic support of the chamber		
h_k	mm	115	a_R	mm	450	k_ξ	N/m	52525
l_c	mm	110	h_R	mm	0	k_η	N/m	13817
l_p	mm	380	J_{cR}	kg·m ²	6.67	b_ξ	N·s/m	14.12
h_{R2}	mm	292.5	J_{cW}	kg·m ²	0.0048	b_η	N·s/m	7.24
a_{R2}	mm	292.5	$k_\xi = k_{\xi_1} = k_{\xi_2} = k_{\xi_3} = k_{\xi_4}$			$b_\xi = b_{\xi_1} = b_{\xi_2} = b_{\xi_3} = b_{\xi_4}$		
β_0	rad	0.785	$k_\eta = k_{\eta_1} = k_{\eta_2} = k_{\eta_3} = k_{\eta_4}$			$b_\eta = b_{\eta_1} = b_{\eta_2} = b_{\eta_3} = b_{\eta_4}$		

On the bases of the derived equations and at the application of parameters concerning the prototype (Table 1), the series of simulation investigations were performed. They were aimed at the determination of the similarity degree of the theoretical analyses results with the experimental tests results, thus, at the verification of the model usefulness.

The results of the computer simulations, corresponding to the performed experiment, are presented in Figures 3 - 6. In this experiment, drive motors of vibrators were uniformly accelerated from the stoppage to the rated speed, by means of the frequency inverter.

The pathways of the power supply frequency of drive motors are shown in Figure 3, while pathways of coordinates of mass centres of the chamber and frame in Figures 4 and 5. The antiresonance zone is clearly seen at the power supply frequency of 50Hz (54-nd second of a simulation), in both directions. At this point the vibration amplitude of the chamber obtained the level of 3 mm. The motion trajectory of the chamber and frame mass centres in the antiresonance work state is presented in Figure 6. In accordance with the expectations this trajectory is of a circular shape.

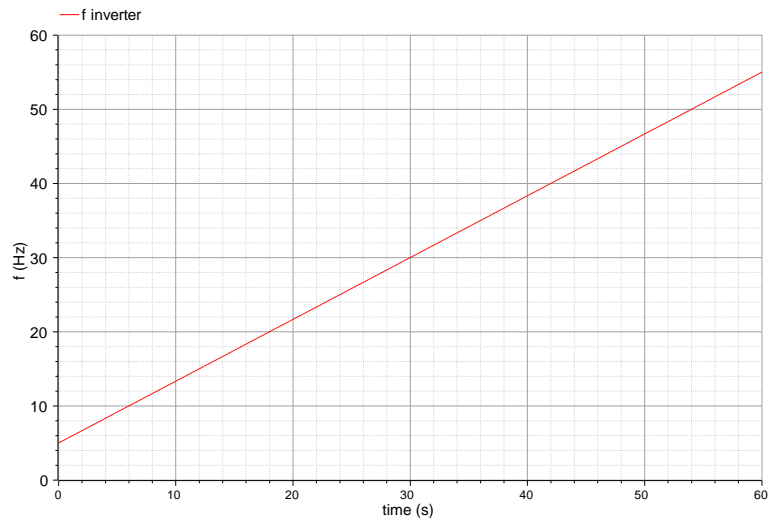


Figure 3. Frequency pathways at the output of the inverter

3. Experiment

Verifying investigations were performed for the vibrations frequencies within the range: 31 to 50 Hz. It should be noticed, that mechanical quantities have 3-times lower frequency value due to utilising 6 pole motors in electrovibrators. Measurements of accelerations for individual frequencies of the frame and chamber were performed by two piezoelectric accelerometers placed on the chamber and on the frame of the mill. The obtained measurements results for the vertical direction are shown in Figure 7, while for the horizontal direction in Figure 8.

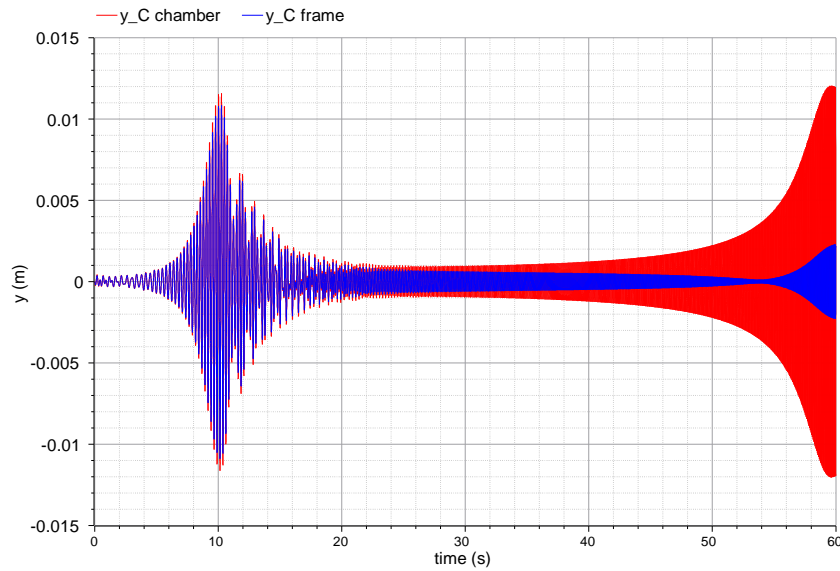


Figure 4. Pathways of coordinate y (vertical direction) of the chamber and frame mass centres during increasing the power supply frequency of drive motors

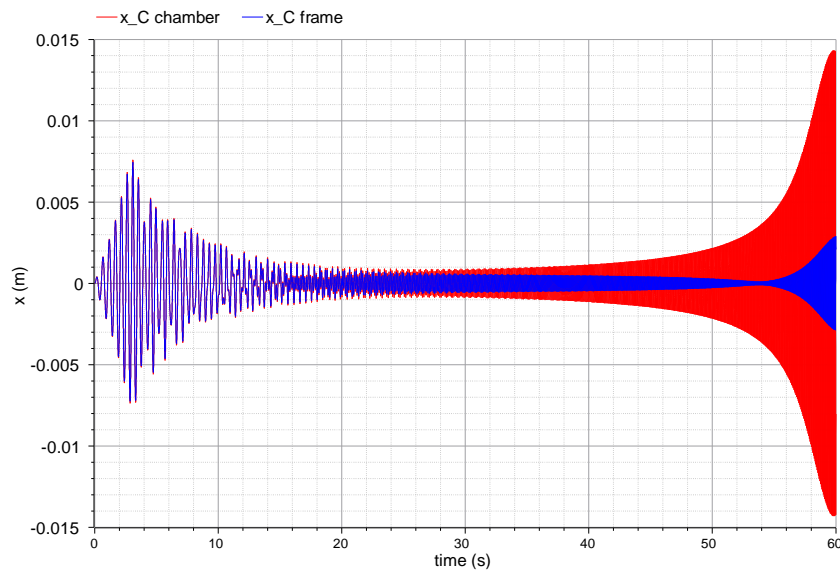


Figure 5. Pathways of coordinate x (horizontal direction) of the chamber and frame mass centres during increasing the power supply frequency of drive motors

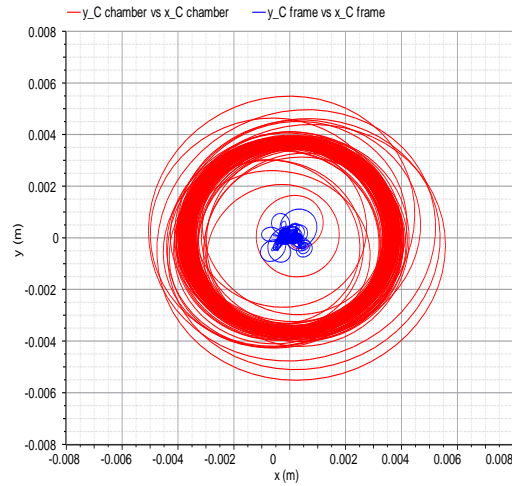


Figure 6. Course of the trajectory of the chamber and frame mass centres in the steady state phase

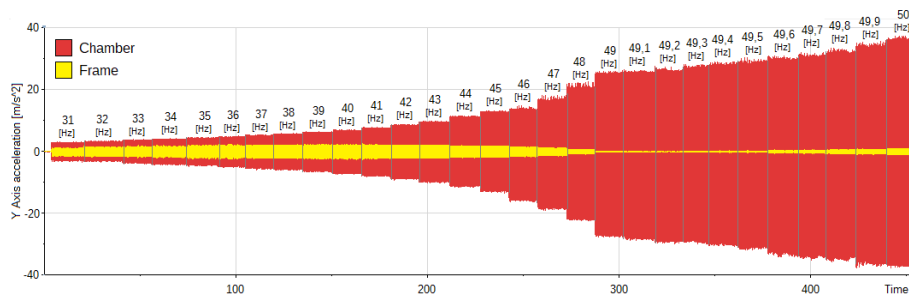


Figure 7. Measurement results y (vertical direction)

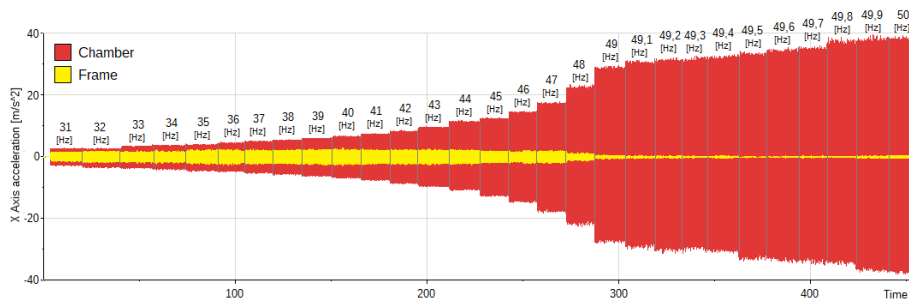


Figure 8. Measurement results x (horizontal direction)

Detailed pathways of the frame and chamber accelerations in the antiresonance zone, corresponding to the frequency value of 49.3 Hz in diagrams 7 and 8, are presented in Figure 9 – for the vertical direction and in Figure 10 - for the horizontal direction.

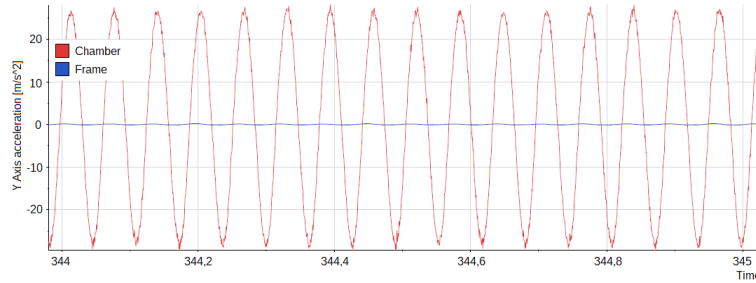


Figure 9. Measurement results of operation in the antiresonance state for the vertical direction

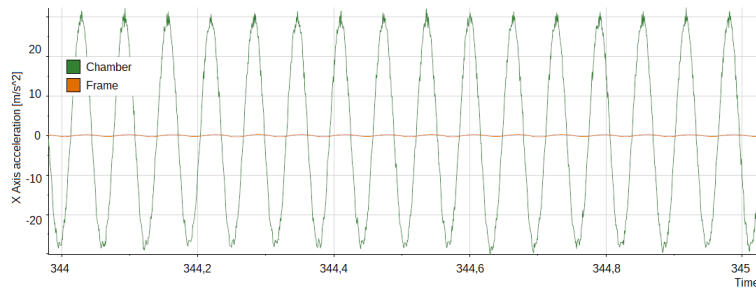


Figure 10. Measurement results of operations in the antiresonance state for the horizontal direction

The chamber trajectory for operations within the antiresonance zone corresponding to the frequency value of 49.3 Hz, from diagrams 9 and 10, is presented in Figure 11.

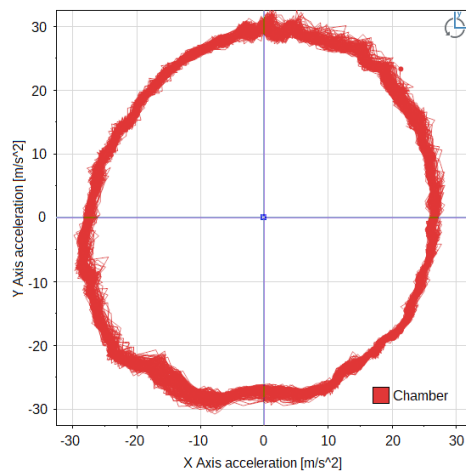


Figure 11. Trajectory of the chamber motion

4. Conclusions

The new solution of the vibration mill of a circular trajectory of the chamber motion, in which the effect of antiresonance was utilised to decrease dynamic influences on foundations or on supporting structures, is presented in the hereby paper. The dynamic equations of the system motion were derived and on their bases simulation tests, aimed at the verification of the assumed - at a designing stage - effects of the device operation, were carried out. In this way, the existence of the total antiresonance of the frame was revealed. It was displayed by a strong reduction of frame vibrations in vertical and horizontal directions (as well as without angular vibrations). The existence - at this stage - the chamber vibrations at a useful level, was also shown. The circular trajectory course of the motion of mass centres of the chamber and frame in the antiresonance work state, was confirmed. Results of simulation analyses were experimentally verified at the specially prepared - for this aim - research set-up. A compatibility of pathways of amplitude-frequency characteristics within the range of possible operations of the device, was found. Moreover, the difference in the antiresonance frequencies was below 1%. A significantly larger difference, of app. 30 %, was detected in amplitude values of frame vibrations in the antiresonance state. Such high discrepancy, the authors explain by inaccurate assessments of damping coefficients of the chamber elastic suspension. Only these parameters, out of all physical parameters, were not determined on the catalogue data or measurements bases. They were determined on the bases of a relative damping coefficient of springs of a similar application. It should be emphasised, that in case of the amplitude of chamber vibrations in the antiresonance state, damping of its suspension plays a significant role [6].

Acknowledgments

The paper was financially supported by: AGH University of Science and Technology under the grant no. 16.16.130.942 for years 2019-2020.

Reference

1. J. Sidor, A. Klich, *Współczesne maszyny do rozdrabniania – kruszarki i młyny*, Instytut Techniki Górniczej KOMAG, Gliwice 2018.
2. E. Gock, K. E. Kurrer, *Eccentric vibratory mills – theory and practice*, Powder Technology, 105 (1999) 302-310.
3. J. Michalczyk, G. Cieplak, J. Sidor, *Numerical simulation model of the rotary-vibrational mill working process*, Archives of Metallurgy and Materials, Polish Academy of Sciences. Committee of Metallurgy. Institute of Metallurgy and Materials Science, 55(1) (2010) 343–353.
4. <https://www.generalkinematics.com/> (29.04.2020)
5. P. Czubak, *Reduction of forces transmitted to the foundation by the conveyor or feeder operating on the basis of the Frahm's eliminator, at a significant loading with feed*, Archives of Mining, 57(4) (2012) 1121–1136.
6. J. Michalczyk, G. Cieplak, *Wysokoefektywne układy wibroizolacji i redukcji drgań*, Collegium Columbinum, Kraków 1999.